

Effect of electrode impedance in improved buffer amplifier for bioelectric recordings

E. R. Valverde*, P. D. Arini, G. C. Bertran,
M. O. Biagetti and R. A. Quinteiro

Cardiac Electrophysiology Laboratory, Department of Physiology, Favaloro University, Argentina

We analysed the effects of electrode impedance on the transfer response of a one-stage improved buffer amplifier. The electrode DC resistance (R_d) modifies the one-stage buffer transfer response. We found a limit electrode resistance ($R_{d(lim)}$) which depends on the transfer damping factor (ε). If R_d is lower than 86.5 k Ω , the transfer response of the buffer fulfils American Heart Association (AHA) recommendations, but when R_d is greater than $R_{d(lim)}$ it must be cautiously weighed up because its influence in the transfer response becomes appreciable. The maximum R_d that can be driven by the buffer is 1.2 M Ω . Higher values do not fulfil AHA recommendations. Therefore, electrodes with higher impedance should not be used with this kind of buffer. In contrast, when this buffer is used to build in an instrumentation amplifier (IA) for bipolar recording, the common-mode rejection ratio (CMRR) is sensitive to the electrode type used.

Nomenclature

$1/\delta$ = Electrode factor
 $A(s)$ = Transfer response as a function of s
 $|A(\omega)|^2$ = Magnitude of the transfer response as a function of ω in dB
 $|A(\omega_{0.14})|^2$ = Magnitude of the transfer response at the frequency $\omega_{0.14}$ in dB
 CMRR = Common-mode rejection ratio
 CMRR_T = Total common-mode rejection ratio from an instrumentation amplifier
 CMRR_B = Input buffer common-mode rejection ratio
 CMRR_D = Differential stage common-mode rejection ratio
 ε = Damping factor
 ε_{min} = Minimum damping factor
 IA = Instrumentation amplifier
 $\phi(\omega)$ = Phase shift of the transfer response as a function of ω in rad s^{-1}
 R_d = Electrode resistance in k Ω
 $R_{d(lim)}$ = Limit electrode impedance in k Ω
 $s_{1,2}$ = Poles of the transfer response
 $\tau_s, \tau_p, \tau_1, \tau_2, \tau_d$ = Time constants in seconds
 ω_0 = Frequency at 0dB in the transfer response in rad s^{-1}
 $\omega_{0.14}$ = The frequency $2\pi \cdot 0.14$ Hz in rad s^{-1}

ω_c = Corner frequency at -3 dB from the flat transfer response in rad s^{-1}

ω_m = Frequency at the peak of the transfer response in rad s^{-1}

ω_n = Natural frequency in rad s^{-1}

Z_e = Electrode impedance

Z_{in} = Input buffer impedance

Introduction

A.c.-coupling and high input impedance are necessary during the amplification of biopotentials during ECG recordings. However, there are several types of electrodes for ECG recording, including metal plate electrodes, recessed electrodes with a sponge immersed in conductive jelly and dry electrodes, all exhibiting different impedance [1–4]. Moreover, the electrode-skin interface and hence electrode impedance could be different for electrodes of the same type when they are applied to unprepared or badly prepared skin. The transfer response of the ECG recorders should be independent of the electrode type used. Commonly, this is achieved by the use of a two-stage op-amp in cascade. The first stage is configured as a unity-gain voltage follower because of its very high input impedance, and the second stage acts like a single high pass filter to arrest the direct component. It has been proposed recently [5, 6] that by combining high input impedance and a.c.-coupling in only one-stage, an improved buffer that fits AHA recommendations [7, 8] can be obtained. Two blocks of this buffer connected to a differential stage are required to obtain the classical three-stage op-amp IA for bipolar recordings. In the present study we analysed the effects of electrode impedance on the transfer response of the one-stage improved buffer amplifier. We showed that the electrode impedance could be represented by a single resistance, R_d , and its value could be of the same order of magnitude as that of the input buffer impedance, driving the buffer transfer response outside of AHA recommendations. We have also shown that the transfer response of the buffer will fall inside the range stated in the AHA recommendations when the improved buffer parameters are recalculated considering the electrode resistance. Further, we analysed the CMRR, when this buffer is used to build an IA for bipolar recordings. Finally, we have also shown that the CMRR decreases when the imbalance of R_d increases and when the resistance of both electrodes are also increased.

*Author for correspondence. Castros Barros 108 9° B CP(1178) Buenos Aires, Argentina; e-mail: estebanvalverde@hotmail.com

Circuit description and analysis

Input stage analysis

The well-known electrode impedance equivalent circuit (Z_e) [3, 4] was represented as shown in figure 1 and has the following transfer response:

$$Z_e(s) = R_d \frac{s\tau_s + 1}{s\tau_p + 1} \quad (1)$$

where $\tau_s = C_s R_s$ and $\tau_p = C_s (R_s + R_d)$. R_d represents the DC component. R_s and C_s represent the Warburg impedance component.

This circuit has a pole and a zero at $1/\tau_p$ and $1/\tau_s$ for low and high frequencies respectively. The input impedance (Z_{in}) of the improved buffer presented by Pallás-Areny *et al.* [5, 6] is given as:

$$Z_{in}(s) = 1/sC_2 + R_1 + R_2 + sC_1 R_1 R_2 \quad (2)$$

The equivalent impedance for ECG electrodes (plates, recessed, dry, etc) were calculated from their frequency response curves [2–4], as shown in figure 2. Z_{in} was calculated with the values proposed by Pallás-Areny *et al.*

In figure 2, it can be seen that at very low and high frequencies the magnitude of Z_{in} is higher than Z_e . However, at intermediate frequencies, where the input impedance of the buffer is $R_1 + R_2$, this value could be of the same order as R_d . Also, it can be seen that the magnitude of Z_e is flat between 0.01 and 100 Hz and the Warburg impedance component becomes appreciable above 100 Hz. In consequence, considering the AHA recommendations, only the DC electrode component could be considered to represent the electrode impedance for analysis of this buffer circuit in the bandwidth stated above. As R_d can hold values of the same order of magnitude as $R_1 + R_2$, these resistances must be taken in account in the buffer design because they could modify its transfer response.

The improved circuit buffer, which includes R_d , is shown in figure 3. The total transfer function is:

$$A(s) = \frac{s\tau_2(1 + s\tau_1)}{1 + s(\tau_2 + \tau_d) + s^2\tau_1\tau_2} \quad (3)$$

where $\tau_1 = (R_1 \parallel R_2) C_1$, $\tau_2 = (R_1 + R_2) C_2$ and $\tau_d = R_d C_2$.

We assumed that only low frequencies are of interest, so the high-order poles of the transfer function are not considered. It can be noticed that the positive feedback through C_1 , R_1 and R_2 acts like an inductor. In consequence, the denominator of equation (3) is a second order polynomial. The damping factor of this second order polynomial is represented by ε , and the natural frequency (ω_n) given by the following expressions:

$$\varepsilon = \frac{(\tau_2/\tau_1)^{1/2}}{2} \quad (4)$$

$$\omega_n = \frac{1}{(\tau_1\tau_2)^{1/2}} \quad (5)$$

The presence of R_d includes an electrode factor ($1/\delta$) that depends on τ_d , and this factor modifies the total

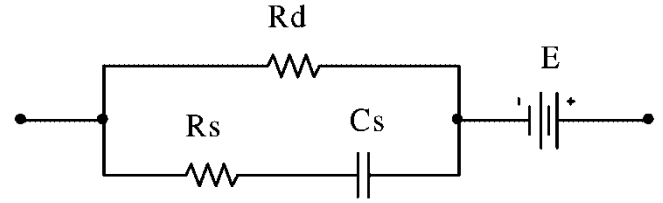


Figure 1. Electrode impedance model circuit. The parallel resistor (R_d) represents the DC component through the electrode-skin interface, the capacitor (C_s) in series with the resistor (R_s) represents the Warburg equivalent for an electrode-skin interface, including the half-cell potential (E).

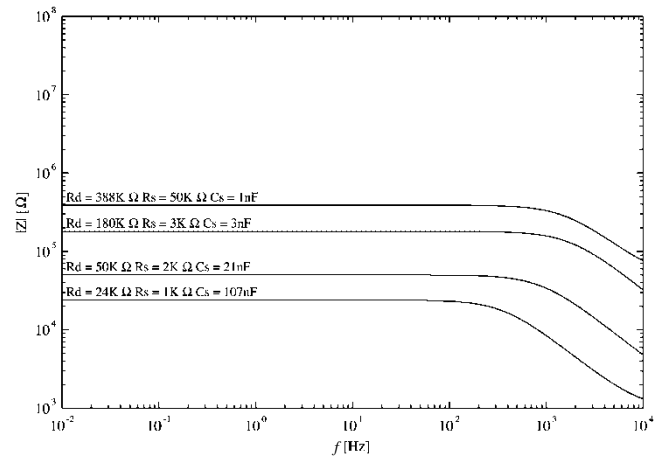


Figure 2. Relationship between different electrode magnitude impedance (Z_e) (solid lines) and input buffer impedance (Z_{in}) (dotted line) at different frequencies. Values obtained for Z_e are shown on each curve. Values for Z_{in} obtained for Pallás-Areny *et al.* [5] are $R_1 = R_2 = 720 \text{ k}\Omega$, $C_1 = 650 \text{ nF}$ and $C_2 = 2 \text{ }\mu\text{F}$.

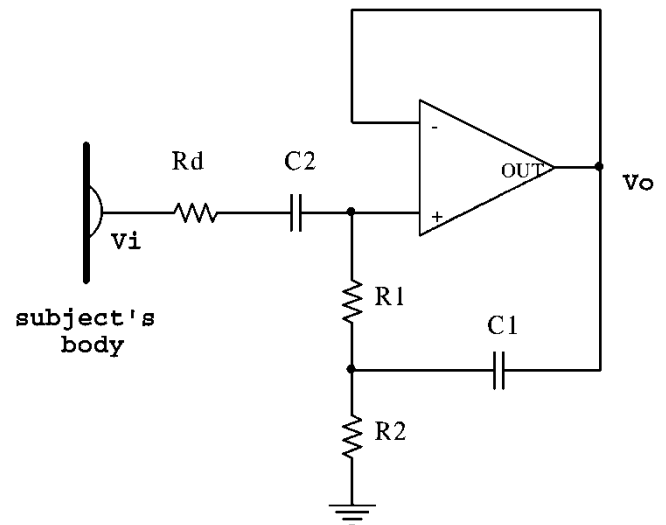


Figure 3. Schematic circuit model of a one-stage buffer op-amp including the electrode DC component (R_d).

damping factor of the transfer response of the second order system, and is given by:

$$\frac{1}{\delta} = 1 + \frac{\tau_d}{\tau_2} \quad (6)$$

The magnitude and the phase of the modified transfer function, considering expressions (4–6), are given by:

$$|A(\omega)|^2 = \frac{\omega^2(\omega^2 + 4\varepsilon^2\omega_n^2)}{(\omega_n^2 - \omega^2)^2 + 4(\varepsilon^2/\delta^2)\omega_n^2\omega^2} \quad (7)$$

$$\phi(\omega) = \tan^{-1} \left[\frac{2\varepsilon\omega_n(\omega^2(1/\delta - 1) + \omega_n^2)}{\omega(\omega_n^2(4\varepsilon^2/\delta - 1) + \omega^2)} \right] \quad (8)$$

Assuming $R_d=0$, then $\tau_d=0$ and therefore equations (3–7) become the same as those proposed by Pallás-Areny *et al.* [5]. Therefore, for a minimum damping factor, ε_{\min} , of 1.76, values of $R_1 + R_2=1.4 \text{ M}\Omega$, $C_1=650 \text{ nF}$ and $C_2=2 \text{ }\mu\text{F}$ were obtained [5].

The poles of the transfer function are:

$$s_{1,2} = \omega_n \left(\frac{\varepsilon}{\delta} \pm \sqrt{\left(\frac{\varepsilon}{\delta}\right)^2 - 1} \right) \quad (9)$$

By increasing R_d , pole positions are modified. If R_d is not considered in the equations and the poles are supposed to be real, the presence of R_d in a real application separates them from each other.

The transfer function is 0 dB at the frequency ω_0 given by:

$$\omega_0 = \frac{\omega_n}{\sqrt{4\varepsilon^2(1 - 1/\delta^2) + 2}} \quad (10)$$

The transfer function has maximum amplitude at the frequency ω_m given by:

$$\omega_m = \frac{\omega_n \sqrt{\sqrt{1 + 8\varepsilon^2(2\varepsilon^2(1 - 1/\delta^2) + 1)} + 1}}{\sqrt{2}} \quad (11)$$

By examining expressions (6), (10) and (11), it can be observed that greater values of R_d increase the frequency ω_0 and decrease the gain at both ω_m and $\omega_{0,14}$, where $\omega_{0,14}=2\pi \cdot 0.14 \text{ Hz}$. Therefore, it is important to consider that R_d should not drive the gain at $\omega_{0,14}$ to values lower than -0.5 dB . Figure 4 shows the magnitude and the phase of the frequency transfer response at two different values of ε : $\varepsilon = 1.76$ in panels A

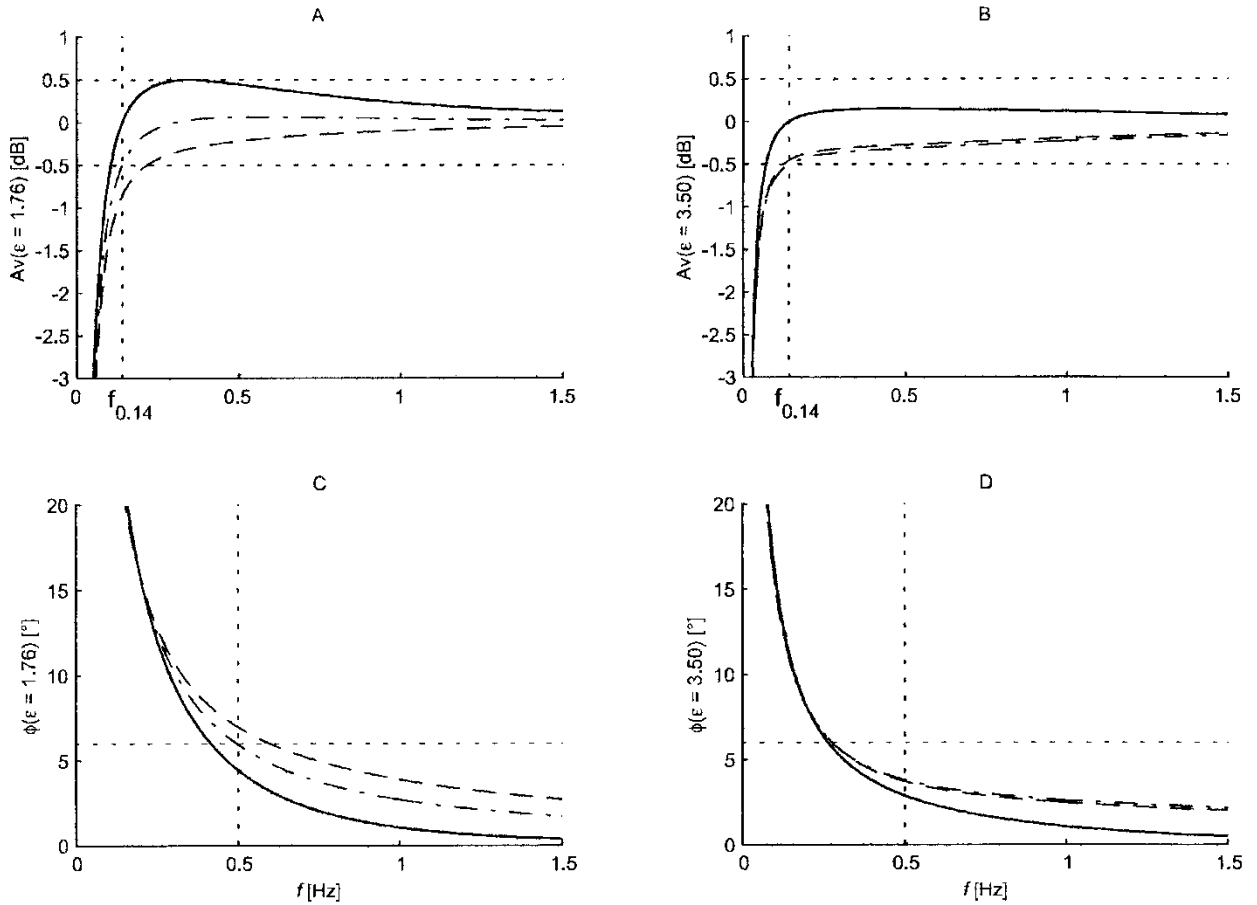


Figure 4. Magnitude and phase transfer response at different values of R_d for $\varepsilon = 1.76$, panels A and C, and $\varepsilon = 3.5$, panels B and D. Solid line indicates the transfer and phase response for $R_d=0 \text{ k}\Omega$, dash-dashed line for $R_d=150 \text{ k}\Omega$ and dot-dashed line for $R_d=R_{d(\text{lim})}$, equal to $86.5 \text{ k}\Omega$ and $167 \text{ k}\Omega$ for each value of ε equal to 1.76 and 3.5, respectively.

and C; and $\varepsilon = 3.5$ in panels B and D, for $R_d = 0$ k Ω and $R_d = 150$ k Ω . In panel A, for $R_d = 0$ k Ω , 0 dB is obtained at $\omega_0 = \omega_{0.14}$ and an overshoot of +0.5 dB can be observed at ω_m . In contrast, for $R_d = 150$ k Ω , the response at $\omega_{0.14}$ is less than -0.5 dB and ω_0 is greater than $\omega_{0.14}$. In panel C, for $R_d = 150$ k Ω , the phase shift is higher than 6° at 0.5 Hz. Because of these conditions, an undershoot can be observed in panel A and the total response falls outside of the AHA recommendation. However, when ε is increased, in panels B and D, the transfer for both $R_d = 0$ k Ω and $R_d = 150$ k Ω satisfy the AHA recommendations.

$R_{d(\text{lim})}$ was calculated from expressions (7) and (10). If R_d is not considered, expression (10) becomes $\omega_n = \omega_0\sqrt{2}$ and $\omega_0 = \omega_{0.14}$ for $\varepsilon = \varepsilon_{\text{min}}$. Replacing these in equation (7), and considering the presence of R_d , the gain at this frequency, $|A(\omega_{0.14})|^2$, starts to decrease and the following expression is obtained:

$$1/\delta = \sqrt{\frac{8\varepsilon^2 + 1 - |A(\omega_{0.14})|^2}{8\varepsilon^2 |A(\omega_{0.14})|^2}} \quad (12)$$

Considering $\varepsilon = \varepsilon_{\text{min}}$ and the limit gain of -0.5 dB, it may be assumed that $1 - |A(\omega_{0.14})|^2 \leq 8\varepsilon_{\text{min}}^2$, therefore, from expressions (6) and (12), the following equation is obtained:

$$R_1 + R_2 \cong \frac{R_d}{\sqrt{\frac{1}{|A(\omega_{0.14})|^2} - 1}} = 16.8R_d. \quad (13)$$

This expression shows that, as R_d increases, $R_1 + R_2$ must be increased too. In figure 4 the transfer response is shown for $R_d = R_{d(\text{lim})}$ (dot-dashed line) in all the panels. In panel A, it can be seen that ε_{min} corresponds to the minimum $R_{d(\text{lim})}$, equal to 86.5 k Ω , estimated from expression (6) and (12), considering $R_1 + R_2 = 1.4$ M Ω . Lower values of electrode resistance do not need to be considered in the design, because the magnitude and the phase transfer response always satisfies AHA recommendations. Moreover, considering the highest resistor values, $R_1 = R_2 = 10$ M Ω , from expression (13), the highest R_d driven by the buffer is 1.2 M Ω .

The corner frequency (ω_c), where the attenuation of the transfer function is no more than 3 dB with respect to the flat transfer response, is given by:

$$\omega_c = \omega_n \sqrt{\sqrt{[2\varepsilon^2(2 - 1/\delta^2) + 1]^2 + 1} - [2\varepsilon^2(2 - 1/\delta^2) + 1]} \quad (14)$$

Figure 5 shows ω_c (left axis) and ε (right axis) both as a function of R_d (solid lines). The dotted line represents the relationship between ε and R_d when $R_d = R_{d(\text{lim})}$. In this figure, when $\varepsilon = 176$, values of R_d greater than $R_{d(\text{lim})}$, determine an increase in the frequency ω_c and the gain at $\omega_{0.14}$ becomes less than -0.5 dB. This behaviour makes the transfer response to fall outside

the AHA recommendations, as it is show in figure 4. In contrast, values of R_d lower than $R_{d(\text{lim})}$ cause the frequency ω_c to decrease and the gain at $\omega_{0.14}$ to become greater than -0.5 dB, maintaining the transfer response within the AHA recommendations. In figure 5, when ε is chosen to obtain a particular ω_c in the buffer design (point **a**) and the electrode impedance is not considered, the presence of R_d in the real application (point **b**) moves ω_c to a higher value (point **c**). In order to maintain the transfer response according to the AHA recommendations, it is necessary to increase ε , for example $\varepsilon = 3.5$, (point **d**) decreasing in consequence the value of ω_c (point **e**).

The following example illustrates all the considerations stated above. Let us suppose that a buffer for the ECG signal is desired with an input impedance higher than 100 M Ω at 50 Hz, a flat response within ± 0.5 dB between 0.14 and 25 Hz and no more than 6° of phase lag at 0.5 Hz. If no electrode resistance is considered and ε_{min} is chosen, $\omega_c = 0.052$ Hz can be obtained by using the component values proposed by Pallás-Areny *et al.* [5] (point **a** in figure 5). Considering $R_d = 150$ k Ω in the real application, ω_c rises to 0.059 Hz (point **c**), the gain at $\omega_{0.14}$ falls to -0.85 dB and the phase lag at 0.5 Hz is greater than 6° , as it is shown in figure 4, panels A and D. From figure 5, it can be deduced that ε will be ≥ 3.5 , hence must be equal to 3.5 (point **d**) in order to maintain the time constant of the buffer as small as possible. From equation (12), $R_1 + R_2 = 2.52$ M Ω . In order to use resistors with the lowest possible values, $R_1 = R_2 = 1.26$ M Ω . From equation (2), 100 M $\Omega \geq \omega_i C_1 R_1 R_2$. For $\omega_i = 314$ rad s $^{-1}$, then $C_1 = 0.19$ μ F. Finally, from equation (4), $C_2 = 2.32$ μ F. The closest commercial values are: $R_1 = R_2 = 1.2$ M Ω , $C_1 = 0.22$ μ F and $C_2 = 2.2$ μ F. These values gives: $Z_{\text{in}}(50 \text{ Hz}) = 99.5$ M Ω , $f_c = \omega_c / 2\pi = 0.031$ Hz, $|A(\omega_{0.14})|^2 = -0.5$ dB and flat response within ± 0.5 dB between 0.14 and 25 Hz is achieved with a phase shift lower than 6° at 0.5 Hz.

Common-mode rejection analysis

The total common-mode rejection ratio (CMRR_T) in an IA for a bipolar recording is:

$$\frac{1}{\text{CMRR}_T} = \frac{1}{\text{CMRR}_B} + \frac{1}{\text{CMRR}_D} \quad (15)$$

where CMRR_B represents the relationship between the gain from the differential input to differential output with respect to the conversion from the common mode input to differential output via the input stages and CMRR_D represents the common-mode rejection ratio of the differential stage of the IA. CMRR_B can be written as follows:

$$\text{CMRR}_B = 0.5 \frac{A_2(s) + A_1(s)}{A_2(s) - A_1(s)} \quad (16)$$

where $A_1(s)$ and $A_2(s)$ represents equation (3) for each input stage of the IA (see [6] for details). On the other hand, CMRR_D depends on the passive components of

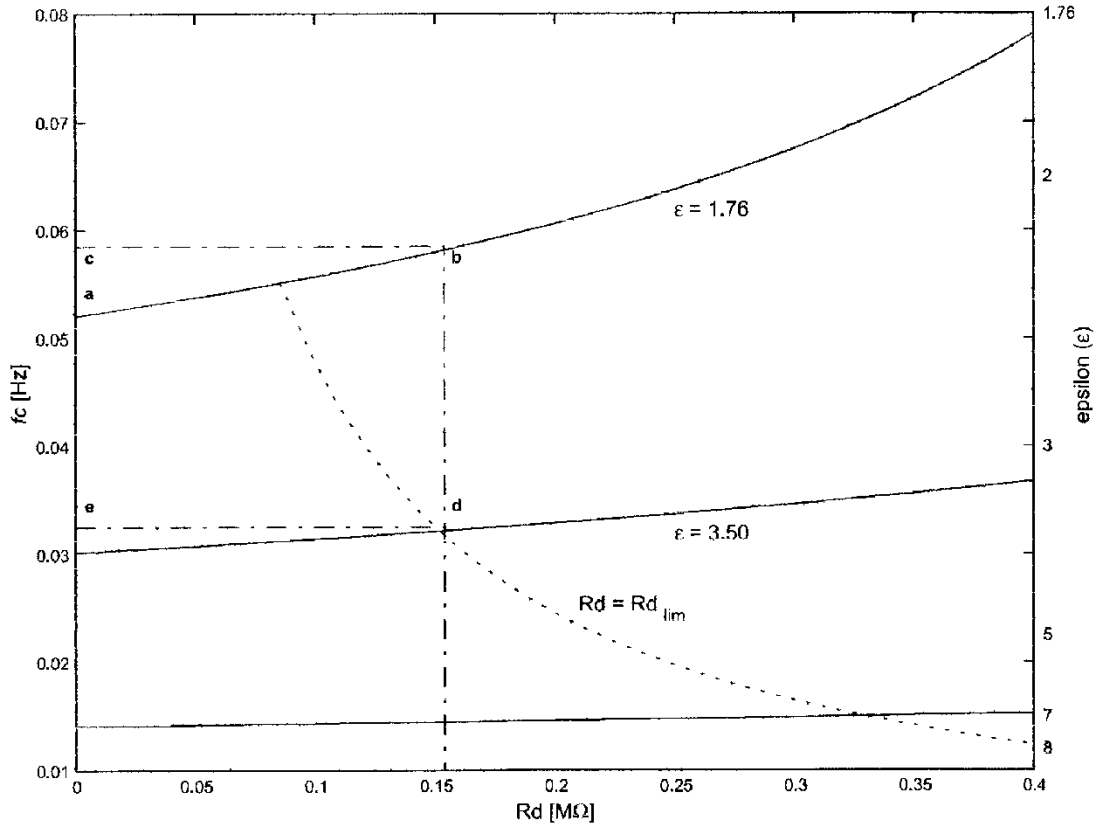


Figure 5. $f_c = \omega_c/2\pi$ (left axis) and ϵ (right axis) as a function of R_d (solid lines). Dotted line represents the relationship between ϵ with $R_d = R_{d(lim)}$. The meaning of points *a* to *e* are fully explained in the text.

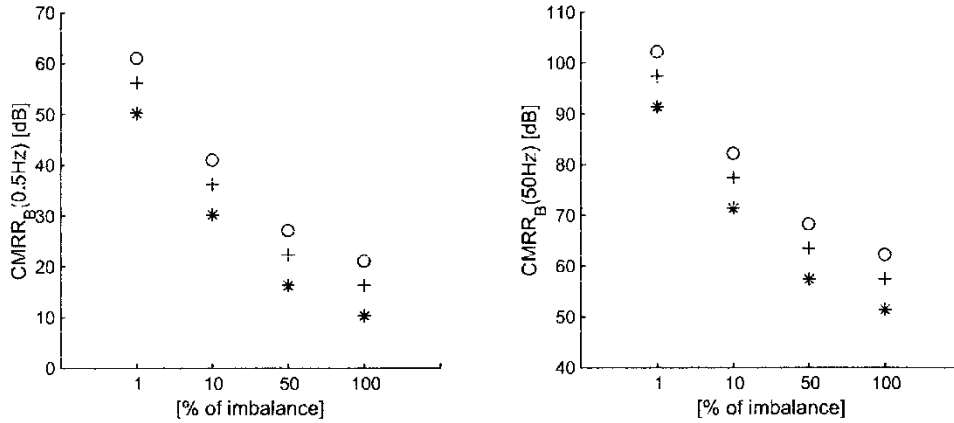


Figure 6. $CMRR_B$ at 0.5 Hz (left panel) and 50 Hz (right panel) for three electrode resistances values as a function of its imbalance. ($\circ = 86.5 \text{ k}\Omega$, $+= 150 \text{ k}\Omega$ and $* = 300 \text{ k}\Omega$). These curves were obtained for $\epsilon = 1.76$ but other values of ϵ have produced the same curves at the same frequency.

the differential stage [6], therefore, it will not be considered in the present study. In order to obtain the highest $CMRR_T$, $CMRR_B$ must be as high as possible and this can be obtained when $A_2(s) - A_1(s)$ is close to zero at all frequencies. For very low frequencies, a high $CMRR_B$ is necessary in order to obtain an important reduction of the baseline movement, usually produced by artefacts generated by the displacement of one or both of the electrodes. At power-line frequency and their harmonics, a high $CMRR_B$ is also necessary in order to reduce the induced electromagnetic inter-

ference generated from near sources. Assuming that each first stage has identical op-amps and passive components, the $CMRR_B$, as a function of the imbalance of R_d , represented as a power relationship, is given as follows:

$$CMRR_B = \frac{(\omega_n^2 - \omega^2) + \epsilon^2(1/\delta_1 + 1/\delta_2)\omega_n^2\omega^2}{4\epsilon^2(1/\delta_1 - 1/\delta_2)\omega_n^2\omega^2} \quad (17)$$

where $1/\delta_1$ and $1/\delta_2$ represents the electrode factor for each input stage.

Equation (17) shows that $CMRR_B$ depends on each R_d and any imbalance between them modifies $CMRR_B$. Figure 6 shows $CMRR_B$ at both 0.5 (baseline movement) and 50 Hz, left and right panel, for pairs of electrodes of 86.5, 150 and 300 k Ω , when the imbalance between each pair of electrodes is 1, 10, 50 and 100%, respectively. In this figure it can be noticed that $CMRR_B$ decreases either when the imbalance between both electrodes increases, as expected, or when the resistance of both of them increases. Also, it can be observed that this buffer reduces the power-line interference more than the baseline movement and, in consequence, special considerations must be taken in account when this buffer is designed for uses under exercises conditions. Later analyses of $CMRR_B$ for different values of ε showed no changes in the curves at both frequencies.

Conclusion

In the present manuscript we have shown that R_d modifies the one-stage buffer transfer response. Also, we have demonstrated that there is an $R_{d(lim)}$, which is dependent on the corresponding ε , for any characteristic of the design. We conclude that the value of $R_{d(lim)}$ for the minimum ε is 86.5 k Ω . Below this value, R_d does not need to be considered in the transfer response of the buffer design. The highest value of R_d that can be driven by the buffer was estimated to be 1.2 M Ω . Moreover, for R_d between 86.5 k Ω . and 1.2 M Ω , higher values of ε must be used in order to comply with AHA recommendations. However, this design has the limitation of decreasing the corner frequency as a consequence of an increase in the time constant of the buffer. Finally, when this buffer is used to build-in an IA for bipolar recording, the CMRR analyses showed it to be sensitive to the electrode type used.

Therefore, taking into account the consideration stated above, we conclude firstly that when this buffer is used to build an IA, the properties of the electrodes must be considered in the buffer transfer response design. Secondly, special care in other details such as the choice of electrodes with lower resistances, skin preparation, quality of attachment, etc, must be considered in order to obtain the highest CMRR.

References

1. BETTS, R. P., and BROWN, B. H., 1976, Method for recording electrocardiograms with dry electrodes applied to unprepared skin. *Medical and Biological Engineering*, **5**, 313–315.
2. BURKE, M. J., and GLEESON, D. T., 2000, A micropower dry-electrode ECG preamplifier. *IEEE Transactions on Biomedical Engineering*, **47**, 155–162.
3. GEDDES, L. A., and BAKER, L. E., 1989, Electrodes. In *Principles of Applied Biomedical Instrumentation*, edited by L. A. Geddes and L. E. Baker (New York, USA: John Wiley Interscience), pp. 315–449.
4. NEUMAN, M. R., 1978, Biopotential electrodes. In *Medical Instrumentation. Application and Design*, edited by J. G. Webster (New Jersey, USA: Houghton Mifflin Company), pp. 215–273.
5. PALLÁS-ARENY, R., COLOMINAS, J., and ROSELL, J., 1999, An improved buffer for bioelectric signals. *IEEE Transactions on Biomedical Engineering*, **36**, 490–493.
6. PALLÁS-ARENY, R., and WEBSTER, J. G., 1990, Composite instrumentation amplifier for biopotentials. *Annals of Biomedical Engineering*, **18**, 251–262.
7. PIPBERGER, H. V, ARZBAECHER, R. C., BERSON, A. S., BRILLER, S. A., and SPACH, M., 1975, AHA Committee Report: Recommendations for standardization of leads and of specifications for instruments in electrocardiography and vectorcardiography. *Circulation*, **52**, 11–31.
8. BAILEY, J. J., and BERSON, A. S., 1990, AHA scientific council: Recommendations for standardizations and specifications in automated electrocardiography: bandwidth and digital signal processing. *Circulation*, **81**, 730–739.